Natsuhara Gigen Ltd, 2003. *Leaflet of the Aspin Spinner Magnetometer*. Osaka, Japan.

Molspin Ltd. *Leaflet of the Minispin Fluxgate Magnetometer*. Newcastle on Tyne, England.

Cross-references

Magnetization, Natural Remanent (NRM)
Magnetization, Remanent

STATISTICAL METHODS FOR PALEOVECTOR ANALYSIS

Our concern is with the statistical description of paleomagnetic vectors and the estimation of their mean and variance. These vectors may come from a number of different rock units or archeological samples, representing a range of acquisition times, and be useful for studies of the mean paleomagnetic field and *paleosecular variation*; alternatively, the vectors may come from individual measurements taken from a given rock unit or archeological sample, representing the same moment of acquisition, and be useful for studying the acquisition process itself. Directional data of a particular polarity are usually analyzed with a *Fisher distribution* (1953), and data of mixed polarities are usually analyzed with a *Bingham distribution* (1964). Occasionally, other directional distributions are used. For example, Bingham (1983) considered the projection of a three-dimensional (3D), scalar-variance Gaussian distribution onto the unit sphere, something he called the "angular-Gaussian" distribution. More recently, Khokhlov *et al.* (2001) considered a generalization of the angular-Gaussian distribution, one with a covariance matrix, which they used to analyze directional data from a number of sites. With respect to intensity data, they have traditionally been treated separately from paleodirections, analyzed with normal, log-normal, or gamma distributions. Here, for data of either a particular polarity or of mixed polarities, we summarize these works, and that of Love and Constable (2003), who developed a full-vector, scalar-variance, Gaussian-statistical framework for treating directional and intensity data simultaneously and self-consistently.

The distributions

In our statistical treatment, each paleomagnetic vector $\mathbf{x}$ is considered to be an independent realization occurring in probability according to a statistical distribution. In Cartesian coordinates (X, Y, Z) the probability $P(\mathbf{x})$ that $\mathbf{x}$ lies within the infinitesimal differential volume

$$\mathrm{d}^3\mathbf{x} = \mathrm{d}X\,\mathrm{d}Y\,\mathrm{d}Z \qquad \text{(Eq. 1)}$$

is

$$P(\mathbf{x}) = \int p(\mathbf{x})\mathrm{d}^3\mathbf{x}, \qquad \text{(Eq. 2)}$$

where $p(\mathbf{x})$ is the density function,

$$p(\mathbf{x}) = \frac{\mathrm{d}^3}{\mathrm{dx}^3}P(\mathbf{x}). \qquad \text{(Eq. 3)}$$

With respect to the many different distributions of probability theory, the Gaussian occupies the most prominent position. This is due to the central limit theorem, which, roughly speaking, asserts that the distribution of the sum of independent, identically distributed random variables is approximately Gaussian. This theoretical underpinning is appealing, and, therefore, for the analysis of paleomagnetic vectors, we consider probability-density functions in a Cartesian three-space of orthogonal magnetic-field components consisting of nonzero mean Gaussian distributions. We model vectors recording data of a particular polarity with a unimodal, Gaussian probability-density function defined in terms of a mean paleomagnetic vector $\mathbf{x}_\mu$ and an associated scalar variance σ^2:

$$p_{g_1}\left(\mathbf{x}|\mathbf{x}_\mu,\sigma^2\right) = \frac{1}{(2\pi)^{3/2}\sigma^3}\exp\left[-\frac{1}{2\sigma^2}(\mathbf{x}-\mathbf{x}_\mu)\cdot(\mathbf{x}-\mathbf{x}_\mu)\right]. \qquad \text{(Eq. 4)}$$

We model vectors of mixed polarities with a bimodal, bi-Gaussian probability-density function, which, in Cartesian coordinates, is

$$p_{g_2}\left(\mathbf{x}|\mathbf{x}_\mu,\sigma^2\right) = \frac{1}{2}\left[p_{g_1}(\mathbf{x}|\mathbf{x}_\mu,\sigma^2) + p_{g_1}(\mathbf{x}|-\mathbf{x}_\mu,\sigma^2)\right]. \qquad \text{(Eq. 5)}$$

The relevant paleomagnetic coordinates are spherical, being the familiar quantities of magnetic intensity, inclination, and declination (F, I, D). In this case, the differential volume element is transformed according to

$$\mathrm{d}X\,\mathrm{d}Y\,\mathrm{d}Z \rightarrow F^2\cos I\,\mathrm{d}F\,\mathrm{d}I\,\mathrm{d}D, \qquad \text{(Eq. 6)}$$

and the Gaussian probability-density function is

$$p_{g_1}\left(\mathbf{x}|\mathbf{x}_\mu,\sigma^2\right) = p_{g_1}\left(F,I,D|F_\mu,I_\mu,D_\mu,\sigma^2\right) = F^2\cos I q(\mathbf{x}|\mathbf{x}_\mu,\sigma^2), \qquad \text{(Eq. 7)}$$

where

$$\begin{aligned} q(\mathbf{x}|\mathbf{x}_\mu,\sigma^2) = {} & \frac{1}{(2\pi)^{\frac{3}{2}}\sigma^3} \\ & \times \exp\left[-\frac{1}{2\sigma^2}\left(F\cos I\cos D - F_\mu\cos I_\mu\cos D_\mu\right)^2\right] \\ & \times \exp\left[-\frac{1}{2\sigma^2}\left(F\cos I\sin D - F_\mu\cos I_\mu\sin D_\mu\right)^2\right] \\ & \times \exp\left[-\frac{1}{2\sigma^2}\left(F\sin I - F_\mu\sin I_\mu\right)^2\right]. \end{aligned} \qquad \text{(Eq. 8)}$$

The quantity F_μ is the magnetic intensity, or the Euclidean length, of the mean vector x_μ, and I_μ and D_μ are the inclination and declination of the mean vector. In spherical coordinates the bi-Gaussian probability-density function is

$$\begin{aligned} p_{g_2}\left(\mathbf{x}|\mathbf{x}_\mu,\sigma^2\right) &= p_{g_2}\left(F,I,D|F_\mu,I_\mu,D_\mu,\sigma^2\right) \\ &= \frac{1}{2}F^2\cos I\left[q(\mathbf{x}|\mathbf{x}_\mu,\sigma^2) + q(\mathbf{x}|-\mathbf{x}_\mu,\sigma^2)\right]. \end{aligned} \qquad \text{(Eq. 9)}$$

If we define θ to be the off-axis angle between a particular unit paleomagnetic vector and the mean unit vector,

$$\hat{\mathbf{x}} = \frac{\mathbf{x}}{|\mathbf{x}|} \quad \text{and} \quad \hat{\mathbf{x}}_\mu = \frac{\mathbf{x}_\mu}{|\mathbf{x}_\mu|}, \qquad \text{(Eq. 10)}$$

then

$$\cos\theta = \hat{\mathbf{x}}\cdot\hat{\mathbf{x}}_\mu. \qquad \text{(Eq. 11)}$$

For both the Gaussian and bi-Gaussian cases the vectorial variance is taken to be spherically symmetrical. That is, the three Cartesian vectorial components are assumed to be independent and to have equal

scalar variance. Such a situation is sometimes described as being one of "isotropic" variance. More generally, however, a Gaussian distribution can be defined in terms of a covariance matrix, where the Cartesian vectorial variance is ellipsoidal, the components having possibly different variances and, even, correlation. Such a situation that is sometimes described as being one of "anisotropic" variance. Of course, because the anisotropic distribution has a larger number of degrees of freedom, it will always fit a given dataset at least as well as the isotropic distribution. In either case, however, it is worth remarking that the Gaussian distributions are idealizations. We do not expect that they will fit all paleovector datasets, since the data themselves result from a myriad of physical processes that in all likelihood cannot be completely distilled down to simple mathematical descriptions. Instead, the utility of statistical distributions is as benchmarks for comparison, and in that sense, the isotropic unimodal and bimodal Gaussian distributions, being relatively mathematically simple, are the most practically attractive.

Marginal forms

For paleomagnetic datasets consisting wholly of coincident intensity and directional measurements, the Gaussian distribution (7) and the bi-Gaussian distribution (9) are of obvious utility. However, in most circumstances, paleomagnetic data consist of only parts, or mixtures of different parts, of the full paleomagnetic vector. Then, what we need are the appropriately marginalized probability-density functions corresponding to the underlying Gaussian distributions. So, for example, most paleomagnetic data are only directional, they consist of inclination-declination pairs with no associated absolute paleointensity. To analyze such data we need the joint probability-density function for inclination and declination, obtained by integrating (7) and (9) over all intensities,

$$p_g\left(I, D|I_\mu, D_\mu, (\sigma/F_\mu)^2\right) = \int_0^\infty p_g(F, I, D)\mathrm{d}F. \qquad \text{(Eq. 12)}$$

Alternatively, if we are analyzing data from an azimuthally unoriented borecore, providing (say) intensity-inclination data, then we need the marginal density function

$$p_g\left(F, I|F_\mu, I_\mu, \sigma^2\right) = \int_0^{2\pi} p_g(F, I, D)\mathrm{d}D. \qquad \text{(Eq. 13)}$$

If the data consist only of inclinations then we integrate (13) over all intensities, etc. In each case, we integrate over the vectorial components that are either not available or are not needed. For reference, all required integrations are given in Love and Constable (2003). In Figure S46 we show the intensity, inclination, declination, and off-axis angular distributions corresponding to the Gaussian distribution (7) for a variety of different dispersions and mean inclinations.

Intensity

In recent years the analysis of paleointensity data, be they from within a particular epoch or spanning a much longer geological period of time, has become the subject of increasing interest to researchers. It is useful, therefore, to compare such data to the intensity distribution corresponding to the 3D Gaussian distributions. For both unimodal and bimodal cases the intensity density function is the same, obtained by integrating either (7) or (9) over all angles,

$$p_g\left(F|F_\mu, \sigma^2\right) = \sigma^{-1}\left(\frac{2}{\pi}\right)^{1/2}\left(\frac{F}{F_\mu}\right) \times \exp\left[-\frac{1}{2}\left(\frac{F}{\sigma}\right)^2 - \frac{1}{2}\left(\frac{F_\mu}{\sigma}\right)^2\right]\sinh\left[\frac{FF_\mu}{\sigma^2}\right], \qquad \text{(Eq. 14)}$$

which is a special case of the n-dimensional Rayleigh-Rician distribution. This function is invariant with respect to change in sign of intensity, although, of course, intensity is, by convention, taken to be a positive quantity. As an aside, we note that distributions of this type have application to digital communications and the radar identification of targets surrounded by Gaussian clutter.

Next, it is enlightening to consider the limiting form of the intensity distribution where $\sigma \ll F_\mu$. It is approximately that for a one-dimensional normal distribution,

$$p_n\left(F|F_\mu, \sigma^2\right) = \frac{1}{\sqrt{2\pi}\sigma}\exp\left[-\frac{1}{2}\left(\frac{F - F_\mu}{\sigma}\right)^2\right], \qquad \text{(Eq. 15)}$$

which McFadden and McElhinny (1982) have suggested might be appropriate for paleointensity studies, after truncation of negative intensities. Note that (15) is not a log-normal distribution and it is not a gamma distribution, each of which have been employed on occasion in the analysis of paleointensity data. However, because it is directly linked to the 3D Gaussian distributions (7) and (9), which can be used for directional analyses as well, and because it applies to a complete and proper range of mean intensities and dispersions, (14) is suitable for paleointensity studies, even (say) during periods of reversal when one can expect that the mean intensity would be small, but the vectorial dispersion would be large.

Off-axis angle

For the Gaussian distribution, the marginal density function for off-axis angle is

$$p_{g_1}\left(\theta|(\sigma/F_\mu)^2\right) = \frac{1}{2}\sin\theta\exp\left[-\frac{1}{2}\left(\frac{F_\mu}{\sigma}\right)^2\right] \times \left\{\left[1 + \left(\frac{F_\mu}{\sigma}\right)^2\cos^2\theta\right]\exp\left[\frac{1}{2}\left(\frac{F_\mu}{\sigma}\right)^2\cos^2\theta\right] \times \left[1 + \mathrm{erf}\left[\frac{1}{\sqrt{2}}\left(\frac{F_\mu}{\sigma}\right)\cos\theta\right]\right] + \left(\frac{2}{\pi}\right)^{\frac{1}{2}}\left(\frac{F_\mu}{\sigma}\right)\cos\theta\right\}, \qquad \text{(Eq. 16)}$$

and the marginal density function for off-axis angle corresponding to the bi-Gaussian distribution is just

$$p_{g_2}\left(\theta|(\sigma/F_\mu)^2\right) = \frac{1}{2}\sin\theta\exp\left[-\frac{1}{2}\left(\frac{F_\mu}{\sigma}\right)^2\sin^2\theta\right] \times \left[1 + \left(\frac{F_\mu}{\sigma}\right)^2\cos^2\theta\right]. \qquad \text{(Eq. 17)}$$

For the limiting case where $\sigma/F_\mu \ll 1$, the unimodal off-axis angular probability-density function (16) is approximately

$$p_f\left(\theta|(F_\mu/\sigma)^2\right) \propto \sin\theta\exp\left[\left(\frac{F_\mu}{\sigma}\right)^2\cos\theta\right], \qquad \text{(Eq. 18)}$$

this corresponding to the Fisher distribution so often used by the paleomagnetic community for unimodal directional. For the bi-Gaussian off-axis angular probability-density function (16), and in the same limit, the off-axis angular density function is approximately

$$p_b\left(\theta|(F_\mu/\sigma)^2\right) \propto \sin\theta\exp\left[\frac{1}{2}\left(\frac{F_\mu}{\sigma}\right)^2\cos^2\theta\right], \qquad \text{(Eq. 19)}$$

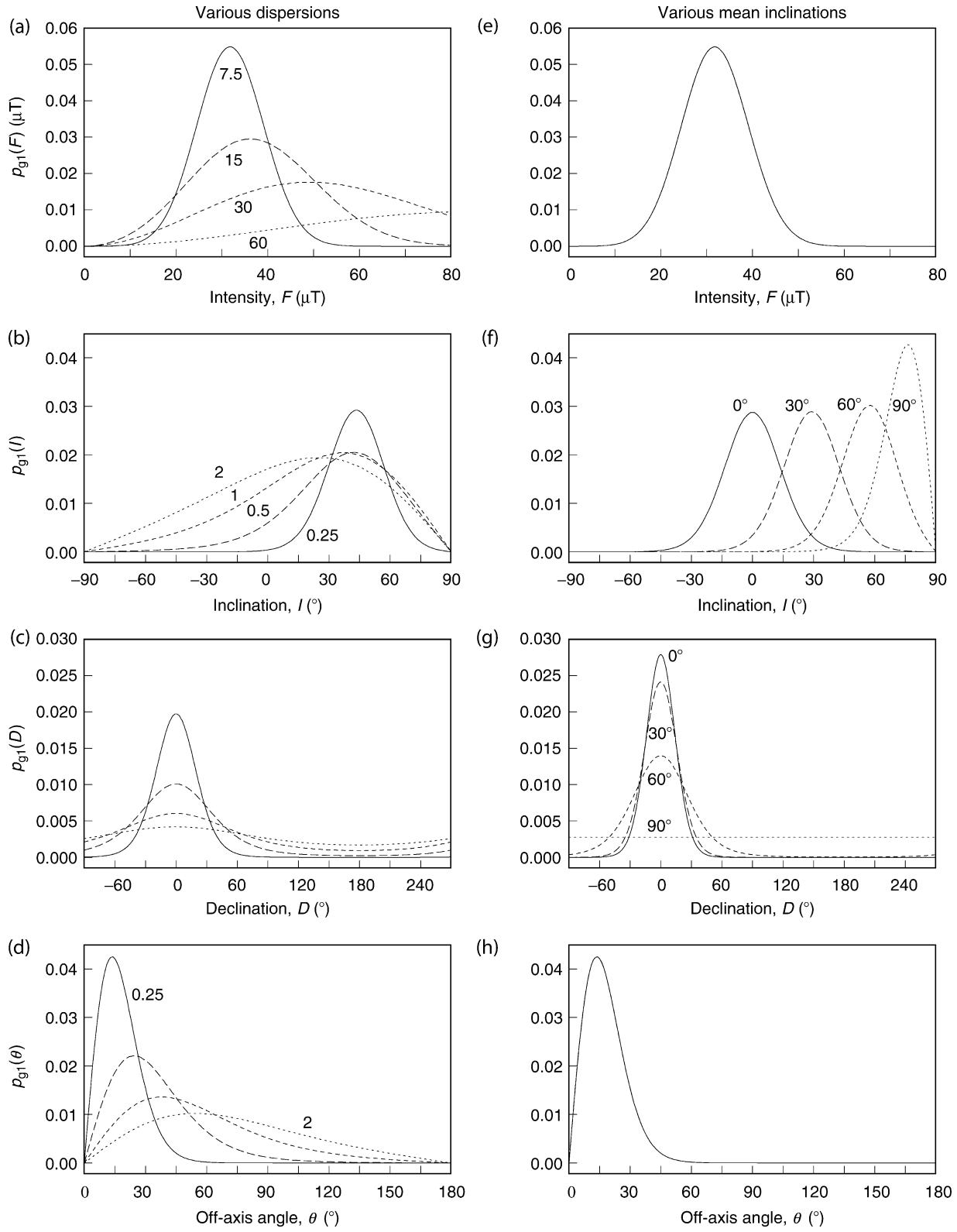

Figure S46 Examples of the marginal probability-density functions p_{g_1} for the Gaussian distribution (7). (a) Intensity F, with vectorial-mean intensity F_μ, and with vectorial dispersions σ of 7.5, 15, 30, and 60 μT, shown, respectively, by solid, long-dashed, short-dashed, and dotted lines. (b) Inclination I, (c) declination D, and (d) off-axis angle θ with vectorial mean direction $(I_\mu, D_\mu) = (45°, 0°)$, and with relative vectorial dispersions σ/F_μ of 0.25, 0.5, 1, and 2, shown, respectively, by solid, long-dashed, short-dashed, and dotted lines. Examples (e-h) are for different mean inclinations, but only the (f) inclination and (g) declination density functions are affected; for vectorial-mean values of $(F_\mu, D_\mu, \sigma) = (30\ \mu T, 0°, 7.5\ \mu T)$ the solid, long-dashed, short-dashed, and dotted lines are for vectorial-mean inclinations I_μ of 0°, 30°, 60°, and 90°, respectively.

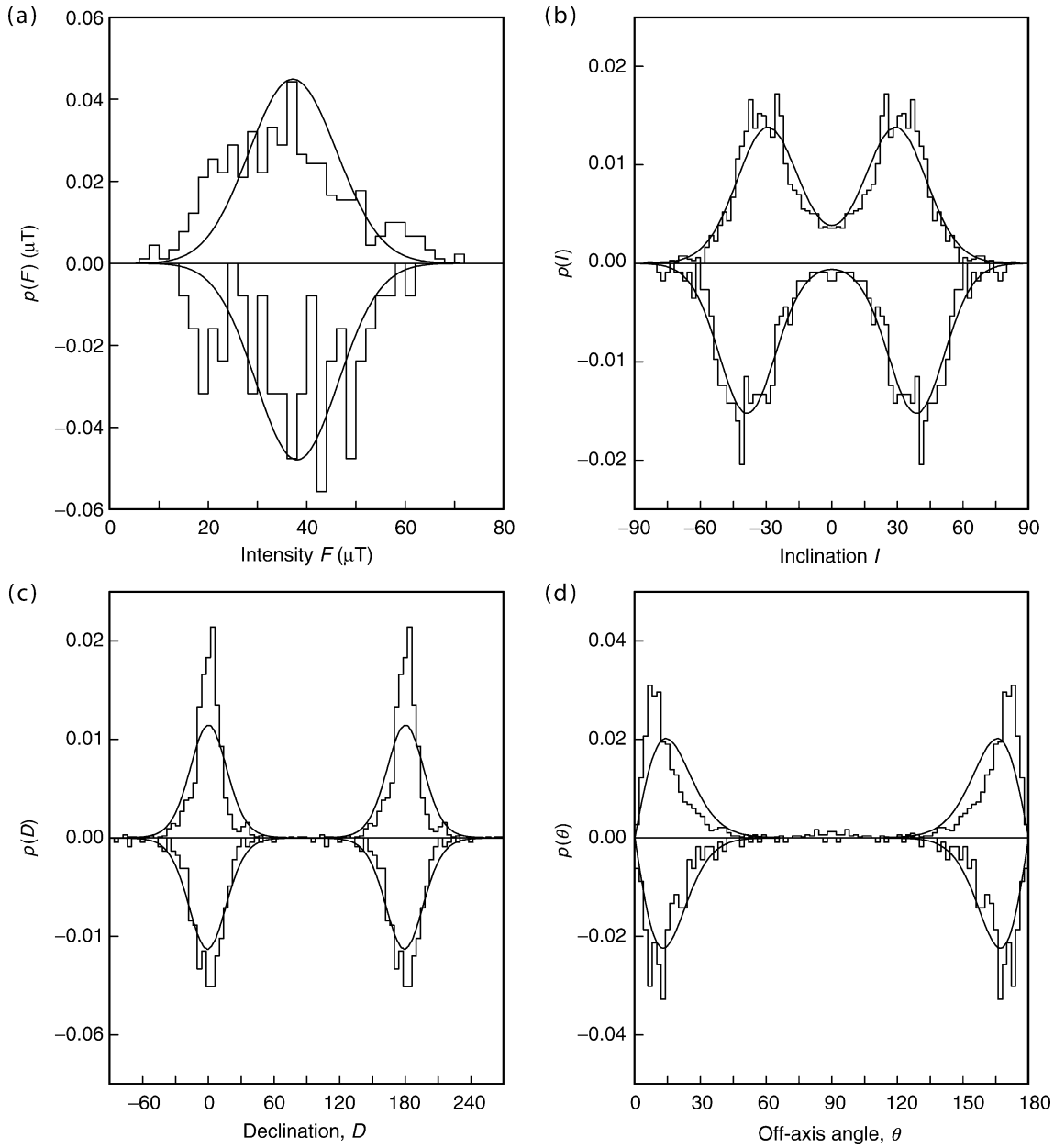

Figure S47 Comparison of maximum-likelihood fits of the 3D bi-Gaussian distribution to the (positive, top) Hawaiian data and (negative, bottom) Réunion data covering the past 5 Ma. Both the probability-density functions and the histograms of the data are shown for (a) intensity, (b) inclination, (c) declination, and (d) off-axis angle. Note that the Réunion data, particularly the declination and off-axis angle data, are fitted better than the Hawaiian data, also note the sizable difference in mean inclination between these two sites.

this corresponding to the Bingham distribution so often used by the paleomagnetic community for bimodal directional analysis. As with our comment about intensity distributions, because they are directly linked to the 3D Gaussian distributions, and because they apply to the complete range of possible vectorial dispersions, (16) and (17) are suitable for most paleodirection studies.

Maximum-likelihood estimation

In fitting paleomagnetic data to a particular Gaussian distribution, thereby yielding a measure of mean and variance, a convenient method is that of maximum-likelihood; for a general review see Stuart *et al.* (1999). With this formalism, the likelihood function is constructed from the joint probability-density function for the existing dataset. In our case we use the Gaussian density functions and/or their appropriate marginalizations to construct the likelihood, which, in its most general form, for all normally encountered types of data groups, is just

$$L = \prod_{j=1}^{N_{FID}} p_g(F_j, I_j, D_j) \prod_{k=1}^{N_{ID}} p_g(I_k, D_k) \times \prod_{l=1}^{N_{FI}} p_g(F_l, I_l) \prod_{m=1}^{N_F} p_g(F_m) \prod_{n=1}^{N_I} p_g(I_n). \quad \text{(Eq. 20)}$$

Here, N_{FID} is the number of intensity-inclination-declination triplets; N_{ID} is the number of inclination-declination pairs, etc. Maximizing L is accomplished numerically (Press *et al.*, 1992), an exercise yielding a particular paleomagnetic vectorial mean and variance. Insofar as the Gaussian distribution is an appropriate description of the paleovector field, then in the limit of large number of data, the maximum-likelihood method yields unbiased estimates of the vectorial mean intensity and the vectorial mean direction (Love and Constable, 2003), which is not usually the case with the traditional method of making separate numerical averages of intensity data and unit directional vectors (Creer, 1983).

Application example

In Figure S47 we show the results (after Love and Constable, 2003) of a maximum-likelihood analysis using the 3D bi-Gaussian distribution and fitting paleomagnetic data covering the past 5 Ma from both Hawaii and Réunion. Comparison of data from these two sites is of interest since they are on almost opposite latitudes, and therefore the asymmetry seen in the data, most prominently in inclination, is indicative of mean-field ingredients other than a simple *geocentric axial dipole*. The Réunion data are fitted much better than the Hawaiian data by the bi-Gaussian distribution with scalar variance, and we can say, therefore, that the Réunion data are relatively "isotropic" in their vectorial variance, while the Hawaiian data display an "anisotropy" in vectorial variance. Better fits to the Hawaiian data would require the introduction of covariance into the underlying Gaussian distribution functions; nonetheless this comparative analysis is enlightening. Software for fitting the 3D Gaussian distributions to paleomagnetic data can be obtained at http://geomag.usgs.gov.

Jeffrey J. Love

Bibliography

Bingham, C., 1964. Distributions on the sphere and on the projective plane. Ph.D. thesis, Yale University, New Haven.

Bingham, C., 1983. A series expansion for the angular Gaussian distribution. In Watson, G.S. (ed.) *Statistics on Spheres.* New York: John Wiley and Sons, pp. 226–231.

Creer, K.M., 1983. Computer synthesis of geomagnetic palaeosecular variations. *Nature*, **304**: 695–699.

Fisher, R.A., 1953. Dispersion on a sphere. *Proceedings of the Royal Society of London, Series A*, **217**: 295–305.

Khokhlov, A., Hulot, G., and Carlut, J., 2001. Towards a self-consistent approach to paleomagnetic field modelling. *Geophysical Journal International*, **145**: 157–171.

Love, J.J., and Constable, C.G., 2003. Gaussian statistics for palaeomagnetic vectors. *Geophysical Journal International*, **152**: 515–565.

McFadden, P.L., and McElhinny, M.W., 1982. Variations in the geomagnetic dipole 2: Statistical analysis of VDMs for the past 5 million years. *Journal of Geomagnetism and Geoelectricity*, **34**: 163–189.

Press, W.H., Teukolsky, S.A., Vetterling, W.T., and Flannery, B.P., 1992. *Numerical Recipes.* Cambridge, UK: Cambridge University Press.

Stuart, A., Ord, K., and Arnold, S., 1999. *Kendall's Advanced Theory of Statistics*, Volume 2A, Classical Inference and the Linear Model. London: Arnold.

Cross-references

Bingham Statistics
Dipole Moment Variation
Fisher Statistics
Geocentric Axial Dipole Hypothesis
Magnetization, Remanent
Nondipole Field
Paleomagnetic Secular Variation
Paleomagnetism

STORMS AND SUBSTORMS, MAGNETIC

Introduction

Magnetic storms were first defined in the mid-19th century when large variations in the horizontal intensity of the magnetic field were measured at a variety of locations on the surface of the Earth. Although much work was subsequently initiated on this topic, it has been the space age that has led to a more detailed understanding of the phenomena involved in magnetic storms. It is now established that magnetic storms are an element of the interaction between processes that occur on the Sun, the coupling between the solar wind and the Earth's magnetosphere, and the subsequent energization of particles within the Earth's magnetosphere (Tsurutani *et al.*, 1997). Furthermore, it is clear that storms occur as a result of abnormal conditions at the Sun and in the solar wind. As a result, the effects during magnetic storms on the space environment surrounding the Earth can be serious in terms of human activities in space and on the ground.

The term "magnetospheric substorm" is used to describe a range of associated phenomena that occur in the magnetosphere. The word substorm was initially used in the early part of the 1960s to portray rapid, repeatable variations of the polar magnetic field during magnetic storms. In order to characterize the overall phenomenology of auroral disturbances, the term was modified to the auroral substorm (Akasofu, 1964), before becoming more widely incorporated as the magnetospheric substorm in the 1970s. Substorms can be considered to be part of the normal solar wind magnetosphere interaction.

Magnetic storms

Magnetic storms are most easily observed in equatorial or low-latitude magnetograms as a depression in the magnetic field. In order to produce a simple means of identifying a magnetic storm, the Dst index was derived, which is based on the change in the horizontal component of the magnetic field measured at a number of low-latitude stations, which are separated in longitude. A schematic representation of the Dst index for an individual storm is given in Figure S48, which illustrates the three specific intervals or phases of a storm, each of which has different timescales.

The initial phase, often but not always, follows a rapid enhancement in the Dst index, over a timescale of a few minutes, which is referred to as a storm sudden commencement (SSC) and is caused by a rapid increase in the solar wind pressure incident on the Earth's magnetosphere.

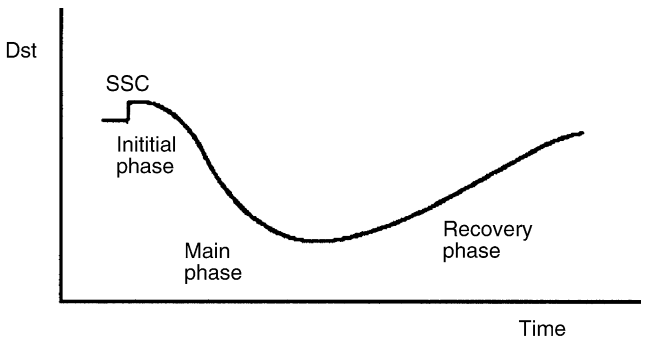

Figure S48 A schematic representation of the Dst index during a typical magnetic storm.